NANO · MICRO small
www.small-journal.com

Sustainable Synthesis of Bimetallic Single Atom Gold-Based Catalysts with Enhanced Durability in Acetylene Hydrochlorination

*Selina K. Kaiser, Adam H. Clark, Lucrezia Cartocci, Frank Krumeich, and Javier Pérez-Ramírez**

Gold single-atom catalysts (SACs) exhibit outstanding reactivity in acetylene hydrochlorination to vinyl chloride, but their practical applicability is compromised by current synthesis protocols, using aqua regia as chlorine-based dispersing agent, and their high susceptibility to sintering on non-functionalized carbon supports at >500 K and/or under reaction conditions. Herein, a sustainable synthesis route to carbon-supported gold nanostructures in bimetallic catalysts is developed by employing salts as alternative chlorine source, allowing for tailored gold dispersion, ultimately reaching atomic level when using H_2PtCl_6. To rationalize these observations, several synthesis parameters (i.e., pH, Cl-content) as well as the choice of metal chlorides are evaluated, hinting at the key role of platinum in promoting a chlorine-mediated dispersion mechanism. This can be further extrapolated to redisperse large gold agglomerates (>70 nm) on carbon carriers into isolated atoms, which has important implications for catalyst regeneration. Another key role of platinum single atoms is to inhibit the sintering of their spatially isolated gold-based analogs up to 800 K and during acetylene hydrochlorination, without compromising the intrinsic activity of Au(I)-Cl active sites. Accordingly, exploiting cooperativity effects of a second metal is a promising strategy towards practical applicability of gold SACs, opening up exciting opportunities for multifunctional single-atom catalysis.

Heterogeneous catalysis by gold is a prime example on the impact of the metal nanostructure on reactivity, a concept that has gained tremendous attention in recent years, particularly in context to single-atom catalysts (SACs), referring to spatially isolated atoms or ions stabilized on a solid carrier.[1] While gold in its bulk form is catalytically inert, supported gold nanoparticles, clusters, and particularly single atoms can unfold remarkable activity for diverse reactions relevant to commodities manufacture, emissions control, and energy conversion.[2] A prominent example is acetylene hydrochlorination, a key technology for the manufacture of vinyl chloride monomer (VCM, 13 Mton y^{-1}), which still runs over highly toxic and volatile mercuric chloride-based catalysts, the use of which will be banned in 2022.[3] Gold SACs stand out as the most active system described to date for this reaction.[3b,4] In comparison, their nanoparticle-based analogs are virtually inactive.[1e,4a] Besides this nuclearity effect, also the coordination environment of the Au single atoms, as defined through interactions with atoms from the host (i.e., C,O) or ligands (i.e., Cl) strongly affects the catalytic response, with Au(I)–Cl single atoms reaching the highest activity. However, owing to the high mobility of Au–Cl single atoms on non-functionalized carbon supports, agglomeration into nanoparticles readily occurs under reaction conditions, leading to catalyst deactivation.[1e,4a] Furthermore, the use of corrosive aqua regia as chlorine-based dispersing agents in typical synthesis protocols,[2b,3b,4a] represents another obstacle in the development of practically applicable Au SACs. To overcome these hurdles, several strategies have been developed to i) replace aqua regia, through the use of sulfur-containing ligands in aqueous solution[5] or non-polar organic solvents,[4b] and ii) increase the catalyst stability through host functionalization (e.g., N-doped carbons, mechanically milled carbon–CeO_2 mixtures),[4a,6] or addition of promoters or second metals.[7] Particularly the latter approach has been widely studied in view of potential bimetallic synergies, stabilizing Au in high oxidation states and balancing HCl and C_2H_2 adsorption. In particular, non-noble metals (e.g., Cu, Ni, Co, Ba, La)[7] and precious metals (e.g., Pt, Pd, Ir, Rh)[8] have been shown to promote and lower the performance of Au-based catalysts in acetylene hydrochlorination, respectively. However, possible correlations to the metal nanostructures were not undertaken at the time, as the structure of the active Au site had not yet been identified. At this time, the metal nanostructure is widely accepted as the key descriptor, determining performance

S. K. Kaiser, L. Cartocci, Dr. F. Krumeich, Prof. J. Pérez-Ramírez
Institute for Chemical and Bioengineering
Department of Chemistry and Applied Biosciences
ETH Zurich
Vladimir-Prelog-Weg 1, Zürich 8093, Switzerland
E-mail: jpr@chem.ethz.ch
Dr. A. H. Clark
Paul Scherrer Institut
Villigen PSI 5232, Switzerland
The ORCID identification number(s) for the author(s) of this article can be found under https://doi.org/10.1002/smll.202004599.

DOI: 10.1002/smll.202004599

in acetylene hydrochlorination, as has further been demonstrated for ruthenium[9] and platinum.[10] Contrary to gold, platinum single atoms exhibits high thermal and chemical stability on carbon hosts and may be prepared via simple incipient wetness impregnation from aqueous solution. In this regard, multimetallic single-atom catalysis may lead to potential synergies. Pioneering work in this direction revealed encouraging catalytic performances in electrocatalytic (i.e., carbon-supported Pt-Ru SAC, denoted as Pt–Ru/C)[11] and organic transformations (i.e., Rh–Ru/CeO_2[12] and Ir–La/C[13]), opening up one of the most recent and intriguing frontiers of the field.[1f] In this contribution, we explore potential synergies between gold and platinum as optimally nanostructured bimetallic SACs, with the aim to enable a greener synthesis (i.e., replacement of aqua regia) and improved stability in acetylene hydrochlorination.

By extrapolating the previously developed synthetic approach to derive carbon-supported Pt SACs (Pt/C) from aqueous solution (nominal metal loading 0.5 weight percent, wt%)[10] to Au/C, large agglomerates form with an average particle size exceeding 70 nm (**Figure 1**a). The origin of this severe agglomeration during the synthesis has been ascribed to the reductive properties of the carbon host and the reduced stability of the gold chloride precursor ($HAuCl_4$) in polar solutions.[4b,14] We demonstrate here that this limitation can be fully overcome through the stoichiometric addition of chloroplatinic acid (H_2PtCl_6), yielding highly dispersed Au–Pt/C catalysts from aqueous solution, as visualized by scanning transmission electron microscopy (STEM) and corroborated by the absence of Au reflections in the X-ray diffraction (XRD) spectrum (Figures S1, S2, Supporting Information). To gain further insight into the nature of the individual metal sites in Au–Pt/C, X-ray absorption spectroscopy (XAS) was employed (for details on the experimental and fitting procedure, see Supporting Information). Comparison of the white-line intensity at around 11 925 eV in the normalized Au L_3-edge X-ray absorption near edge spectrum (XANES), indicated a generally lower degree of highly charged and/or chlorinated metal species, compared to benchmark Au-SA/C prepared from aqua regia (Figure 1b). Fitting of the extended X-ray absorption fine structure (EXAFS), using Au–C/O, Au–Cl and Au–Au/Pt contributions on the Au L_3 edge and Pt–C/O, Pt–Cl and Pt–Pt/Au on the Pt L_3 edge, revealed a decrease in the Au–Cl contribution in the order of Au–SA/C >Au–Pt/C > Au–NP/C (Figure 1c; Figure S3, Table S1, Supporting Information, coordination number, CN = 2.7 ± 0.3, ≈0.9, and 0.4 ± 0.1, respectively). Similar to the Au single atoms, also the Pt sites are surrounded by Cl neighboring atoms (Figure S4, Table S2, Supporting Information, CN = 2.6), suggesting that Cl ions are not removed during the synthesis of the catalyst, in line with previous literature reports[4,12] and corroborated by the surface and bulk chlorine contents derived from X-ray photoelectron spectroscopy (XPS) and elemental analysis, respectively (Table S3, Supporting Information). Besides metal-chloride contributions, the EXAFS fitting results for Au–Pt/C suggest further, the presence of metal–metal interactions (Table S1, Figure S3, Supporting Information). However, owing to an overlap between the Au L_3 and Pt L_3 edges, these results exhibit a high degree of uncertainty and can only suffice as a general guideline. Additionally, due to the virtually undistinguishable Au and Pt scattering paths, it is beyond the scope of this technique to indicate whether the metallic contributions are of mono or bimetallic nature (i.e., Au—Pt or Au—Au bonds). Particularly the presence of low-nuclearity clusters (i.e., dimers, trimers) seems to be a viable possibility, as the latter are virtually indistinguishable by STEM and would not be visible by XRD analysis.[15] Similarly, also STEM electron energy loss spectroscopy (EELS) cannot be employed to gain additional insights into the interaction and/or proximity between the Au and Pt sites, as this technique is only applicable to systems in which the atoms of interest are stationary (i.e., highly stabilized

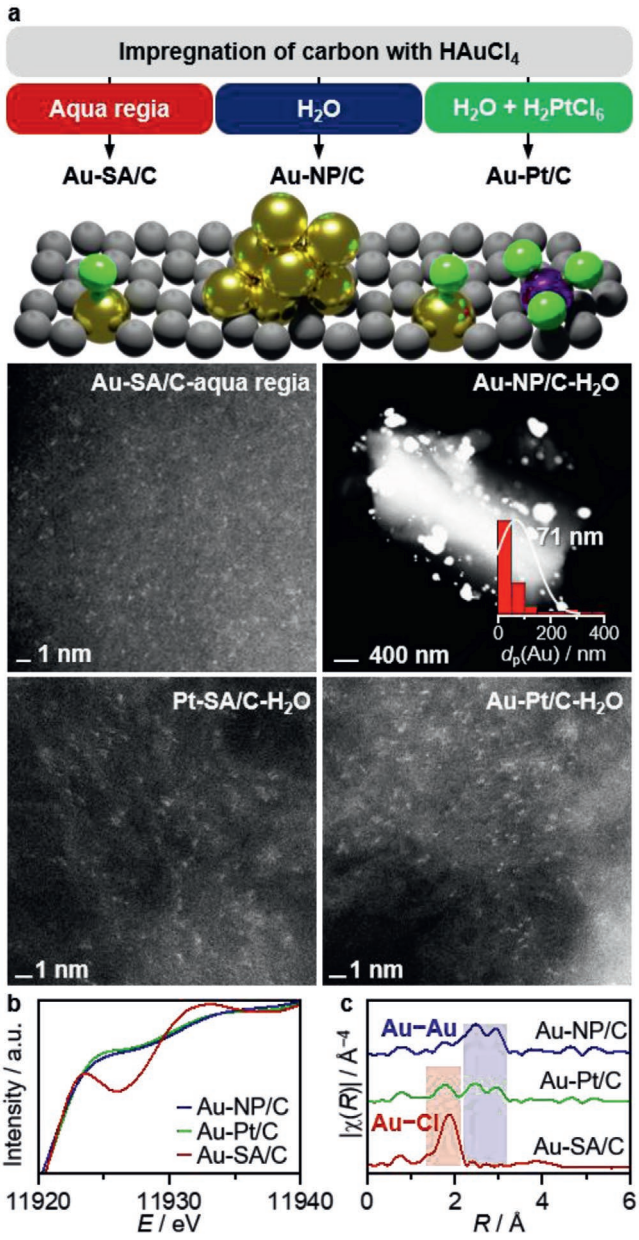

Figure 1. a) Schematic representation of the synthetic routes to carbon-supported Au-, Pt-, and Au–Pt single-atom catalysts. Color code: C, grey; Cl, green; Au, gold; Pt, purple. The STEM images of the mono and bimetallic catalysts visualize the remarkable redispersing effect of platinum chloride, transforming large Au agglomerates into small clusters and single atoms in aqueous solution. b,c) Au L_3 edge XANES and EXAFS spectra.

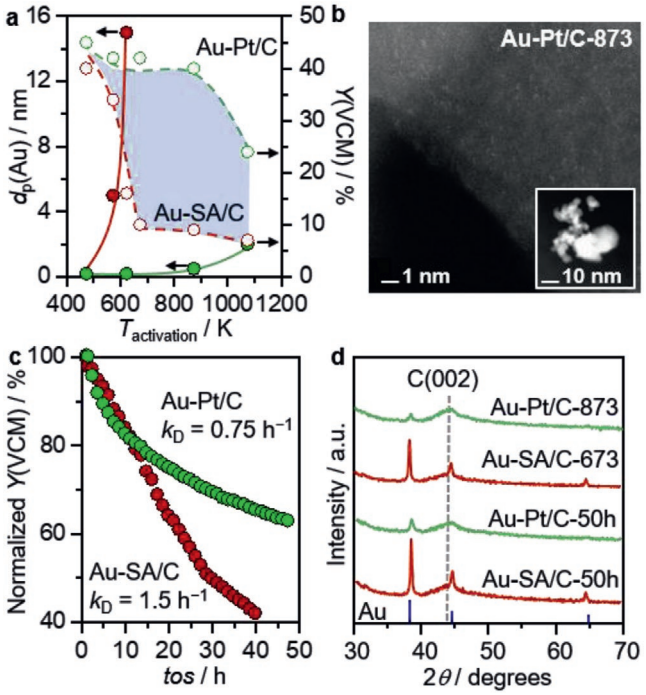

Figure 2. a) Evolution of the Au particle size, derived from STEM analysis in the absence or presence of Pt atoms as a function of the thermal activation temperature and corresponding acetylene hydrochlorination activity, expressed as the yield of VCM. b) STEM image of Au–Pt/C after thermal activation at 873 K, showing predominantly isolated atoms with occasional Au agglomerates (see inset). c,d) Comparison of the stability of Au–SA/C and Au–Pt/C in acetylene hydrochlorination, accompanied by the respective deactivation constants (k_D), and XRD spectra of both catalysts after 50 h time-on-stream (*tos*). Diffraction patterns of metallic Au and graphitic carbon are highlighted with vertical lines, respectively.

on the support) under the electron beam.[16] This is not the case for Au–Cl single atoms on carbon, which are very mobile and readily agglomerate upon prolonged exposure to an electron beam.[4a] In this regard, also XPS analysis is limited by the high susceptibility of Au–Cl single atoms to undergo photoreduction to metallic Au species upon exposure to the incident X-ray beam during acquisition (Figure S5, Table S4, Supporting Information), in line with previous literature reports.[3b,4a] Hence, deeper insights into the interaction and/or proximity between the metal sites remain unsolved since this represents the frontier of what state-of-the art characterization techniques can achieve today.[1f] Thus, it can only be concluded that the degree of Au dispersion is significantly improved in Au–Pt/C compared to benchmark Au–NP/C.

To probe whether this dispersing effect of H_2PtCl_6 can be further exploited to improve the thermal stability of Au atoms on carbon, the benchmark Au/C SAC prepared from aqua regia (denoted as Au–SA/C) and Au–Pt/C were thermally activated at varying temperatures up to 1073 K (N_2 atmosphere, 12 h) and analyzed by STEM. While in the case of Au–SA/C, severe particle agglomeration occurs at temperatures >500 K, exceeding an average particle size of 16 nm at 600 K, the bimetallic counterpart is significantly stabilized, maintaining high dispersion up to 800 K and following afterwards a much slower sintering rate (**Figure 2**a,b). To further corroborate these results, acetylene hydrochlorination was employed as a means to indirectly assess the degree of Au dispersion, taking advantage of the well-known high structure-sensitivity of this reaction (T_{bed} = 473 K, HCl:C_2H_2 = 1.1:1, gas hourly pace velocity based on acetylene $GHSV(C_2H_2)$ = 1500 h^{-1}). At low activation temperatures of 473 K, both Au–Pt/C and Au–SA/C exhibit comparably high initial catalytic activity, as is well in line with the presence of Au single atoms in these samples. However, following thermal activation >600 K, the initial catalytic activity of Au–SA/C sharply drops, while the performance of Au–Pt/C remains high up to activation temperatures of 900 K. Following these encouraging results, we assessed the stability of Au–Pt/C in acetylene hydrochlorination in comparison to Au–SA/C, within 50 h tests ($GHSV(C_2H_2)$ = 560 h^{-1}, Figure 2c). Although both systems gradually deactivate, Au–Pt/C exhibits a ≈2-fold improved stability, which relates well to the significantly reduced sintering of Au under reaction conditions, as evident from STEM and XRD analysis of the used catalysts (Figure 2d; S6, Supporting Information). Notably, the surface area decreased gradually for both catalysts with prolonged reaction time, indicating coking as additional cause of catalyst deactivation (Table S5, Supporting Information). While these results confirm the stabilizing effect of Pt on Au nanostructures, also under reaction conditions of acetylene hydrochlorination, evaluation of the reaction kinetics of Au–SA/C and Au–Pt/C showed only marginal differences (Figure S7, Supporting Information).

This result, in combination with the comparable initial activity of the two catalysts per mole of gold, hints at the predominating role of Au(I)–Cl single atoms as the active site in the bimetallic catalyst, rather than Pt(II)–Cl single atoms, which generally exhibit only half the activity of their Au-based counterparts (Figure S2b, Supporting Information).[12] These assumptions further imply that platinum does not majorly modify the structure of the active Au site and the two metals are too far apart to enable the spillover of reactants (i.e., >5 Å, in neighboring cavities). However, as the agglomeration rate of gold is markedly reduced in the presence of platinum single atoms, we further hypothesize that the latter effectively block the movement of gold in neighboring sites (immediate or close), which is a rather statistical process, while energetic alternations due to proximity are less likely. To further investigate the remarkable stabilization potential of Pt on Au single atoms and assess whether also other metals may be employed in place of Pt, an array of Au-bimetallic catalysts was prepared, using alkali and earth alkaline metal-, non-noble, and precious metal chlorides (Figure S2, Supporting Information). Combination of XRD analysis and evaluation in acetylene hydrochlorination identifies a positive correlation between a reduced Au particle size and the catalytic activity for all bimetallic catalysts, reinforcing Au dispersion as the determining descriptor for initial activity. In particular, combinations with Cu, Rh, Ir, Pd, Zn, and Ni, show enhanced activity compared to Au–NP/C, whereas all other metals exhibit similar or lower (Au–Fe/C) performance. Comparable conversion levels to Au–SA/C were achieved with Au–Cu/C and Au–Rh/C, which is well in line with the high degree of Au dispersion (i.e., presence of single atoms and small nanoparticles with an average particle size of 1.2–1.4 nm, **Figure 3**) in these samples. In the case of Au–Ir/C and Au–Ni/C also larger Au agglomerates were identified, (average particle size

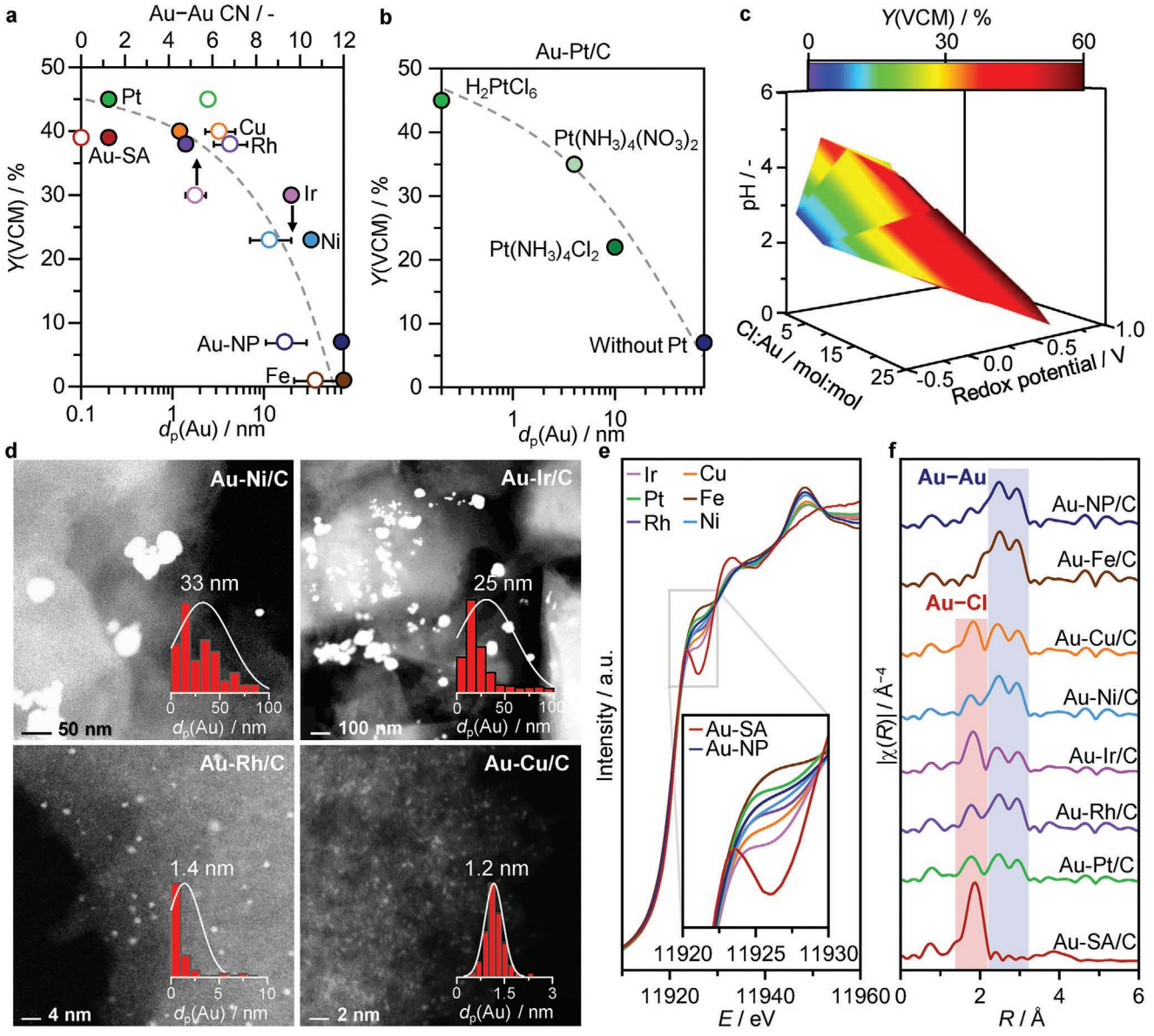

Figure 3. a) Acetylene hydrochlorination performance of selected bimetallic Au-based catalysts as a function of the gold particle size, derived from STEM analysis and EXAFS fitting (Au–Au coordination number). b)Impact of the choice of Pt precursor on the degree of Au dispersion and yield of VCM. c) Correlation between catalytic performance and the redox potential of the second metal, the Cl:Au ratio as calculated from the respective stoichiometry in the metal chlorides, and acidity of the selected metal precursor, as derived from 25 samples (Figure S9, Supporting Information). d) STEM images of selected Au-bimetallic catalysts with average gold particle size distributions, obtained from >100 particles. e,f) Au L_3 edge XANES and EXAFS spectra of selected bimetallic Au-based catalysts in reference to Au–SA/C, Au–Pt/C and Au–NP/C.

25 and 33 nm), co-existing with isolated atoms, small clusters and nanoparticles. Notably, no nanoparticles of the respective second metals were observable in all samples, suggesting the presence of low-nuclearity clusters and/or single atoms. To gain further insights into the nature of the metal sites, their local coordination environment, and possible interactions between different entities, XAS analysis was performed. Inspection of the Au L_3 edge and respective other metal edges indicated the absence of a direct Au—M bond in all samples. Hence, the fitting models were constructed, using Au–C/O, Au–Cl and Au–Au contributions on the Au L_3 edge and M–C/O, M–Cl and M–M on the M edges. In good agreement with the catalytic data and the STEM results, XANES analysis (i.e., comparison of the white-line intensities at 11 925 eV) and EXAFS fitting at the Au L_3 edge suggest the following order of increasing Au–Cl content (decreasing Au–Au contribution): Au–Fe/C < Au–NP/C < Au–Ni/C < Au–Rh/C < Au–Cu/C < Au–Ir/C (Figure 3e,f; Figure S3, Table S1, Supporting Information). Detailed fitting of the respective other metal edges indicates no metal–metal interaction (with the exception of Ni), corroborating the presence of isolated atoms as predominating species (Figure S4, Table S2, Supporting Information). Mostly chlorine-containing atoms were formed, with the notable exception of Cu and Ni, exhibiting only O/C-neighbors, hinting at

the presence of hydrated species. Stability assessment in acetylene hydrochlorination within 12 h tests, revealed an increasing deactivation rate in the order of Au–Pt/C < Au–Ni/C ≈ Au–Cu/C < Au–SA/C < Au–Rh/C ≈ Au–Ir/C (Figure 2c; Figure S8, Supporting Information). Accordingly, due to exhibiting superior initial activity and stability compared to benchmark Au–SA/C at equal loading, Au–Pt/C and Au–Cu/C were identified as the most attractive systems.

Besides the central role of the second metal, also the Au:M molar ratio, the acidity of the MCl_x precursor solution and the availability of chlorine ligands were studied as potential factors, influencing the overall degree of Au dispersion and thus performance in acetylene hydrochlorination (Figure 3b; Figures S6, S9, Supporting Information). Evaluation of these parameters for the whole platform of 25 bimetallic catalysts indicated high catalytic activity, if three factors were fulfilled: i) a high redox potential of the second metal, ii) high acidity of the metal precursor solution, and iii) a large excess of chlorine ligands during the impregnation step, as estimated from the respective Cl:Au stoichiometry in the metal chloride precursor salts (Figure 3c, see the Experimental Section in Supporting Information for details). Under these optimal conditions, large Au agglomerates (i.e., >70 nm in Au–NP/C) can be redispersed on carbon into isolated atoms (or low-nuclearity clusters) through the simple addition of H_2PtCl_6 in aqueous solution (Figure S10, Supporting Information). These observations hint at the key role of Pt in promoting a chlorine-mediated oxidation of reduced Au sites, leading to high Au dispersion and possibly further improving Au stabilization in chlorine-containing atmosphere. In line with this hypothesis, the surface chlorine content of Au–Pt/C, as derived by XPS analysis, increases from 0.18 to 0.86 wt% within 12 h time-on-stream in acetylene hydrochlorination, which is enhanced compared to Au–Cu/C (0.18 to 0.43 wt%) and contrasts the decrease observed for Au–SA/C (1.10 to 0.74 wt%, Table S3, Supporting Information).

In summary, we developed a sustainable and potentially scalable route for the synthesis of carbon-supported gold nanostructures in bimetallic catalysts, employing small amounts of metal salts in aqueous solution as alternative chlorine source to corrosive aqua regia, widely used in previous protocols. Thereby, the choice of metal chloride determines the degree of gold dispersion, ultimately reaching atomic level when using H_2PtCl_6. The possible origin of this remarkable dispersion effect of platinum (and similarly for other metals such as copper), was ascribed to the key role in promoting a chlorine-mediated dispersion mechanism, which can be further exploited to redisperse large gold agglomerates (>70 nm) on carbon carriers into isolated atoms, a phenomenon of practical relevance for catalyst regeneration strategies. We further show for the first time, that in the presence of platinum single atoms, the stability of their gold-based analogs can be increased against sintering up to 800 K, which translates into a two-fold improved lifetime in acetylene hydrochlorination, without compromising on the high catalytic activity of Au(I)–Cl active sites. This observation indicates that the two metals are likely spatially isolated and Pt single atoms effectively block the gold diffusion paths. In this regard, the herein uncovered cooperativity effects have important implications for the frontier of single-atom catalysis and call for further explorations and developments of characterization tools to deepen our understanding on the complex interactions of multimetallic SACs.

Supporting Information

Supporting Information is available from the Wiley Online Library or from the author.

Acknowledgements

This work was supported by ETH research grant ETH-40 17-1. The authors thank Simon Büchele for conducting XPS analyses and Ivan Surin for assistance with catalyst preparation and testing. The Scientific Center for Optical and Electron Microscopy at the ETH Zurich, ScopeM, and the SuperXAS beamline at PSI, are thanked for access to their facilities. The service for Microelemental Analysis at ETH Zurich is acknowledged for chlorine analyses.

Conflict of Interest

The authors declare no conflict of interest.

Keywords

acetylene hydrochlorination, bimetallic catalysts, gold, platinum, single-atom catalysis

Received: July 29, 2020
Revised: October 27, 2020
Published online: January 12, 2021

[1] a) A. Wang, J. Li, T. Zhang, *Nat. Rev. Chem.* **2018**, *2*, 65; b) M. Pagliaro, *Single-Atom Catalysis – A Forthcoming Revolution in Chemistry*, Elsevier, St. Louis, MO **2019**; c) X. Li, Y. Huang, B. Liu, *Chem* **2019**, *5*, 2733; d) X. Li, H. Rong, J. Zhang, D. Wang, Y. Li, *Nano Res.* **2020**, *13*, 1842; e) G. Malta, S. A. Kondrat, S. J. Freakley, C. J. Davies, S. Dawson, X. Liu, L. Lu, K. Dymkowski, F. Fernandez-Alonso, S. Mukhopadhyay, E. K. Gibson, P. P. Wells, S. F. Parker, C. J. Kiely, G. J. Hutchings, *ACS Catal.* **2018**, *8*, 8493; f) S. K. Kaiser, Z. Chen, D. F. Akl, S. Mitchell, J. Pérez-Ramírez, *Chem. Rev.* **2020**, https://doi.org/10.1021/acs.chemrev.0c00576.

[2] a) R. Ciriminna, E. Falletta, C. Della Pina, J. H. Teles, M. Pagliaro, *Angew. Chem., Int. Ed.* **2016**, *55*, 14210; b) C. W. Corti, R. J. Holliday, D. T. Thompson, *Appl. Catal. A* **2005**, *291*, 253; c) S. Ding, M. J. Hülsey, J. Pérez-Ramírez, N. Yan, *Joule* **2019**, *3*, 2897; d) Q. Fu, H. Saltsburg, M. Flytzani-Stephanopoulos, *Science* **2003**, *301*, 935; e) G. J. Hutchings, *Catal. Today* **2005**, *100*, 55.

[3] a) R. Lin, A. P. Amrute, J. Pérez-Ramírez, *Chem. Rev.* **2017**, *117*, 4182; b) G. Malta, S. A. Kondrat, S. J. Freakley, C. J. Davies, L. Lu, S. Dawson, A. Thetford, E. K. Gibson, D. J. Morgan, W. Jones, P. P. Wells, P. Johnston, C. R. Catlow, C. J. Kiely, G. J. Hutchings, *Science* **2017**, *355*, 1399; c) United Nations Environment Programme, Minamata Convention on Mercury, www.mercuryconvention.org/, (accessed: July 2020).

[4] a) S. K. Kaiser, R. Lin, S. Mitchell, E. Fako, F. Krumeich, R. Hauert, O. V. Safonova, V. A. Kondratenko, E. V. Kondratenko, S. M. Collins, P. A. Midgley, N. Lopez, J. Pérez-Ramírez, *Chem. Sci.* **2019**, *10*, 359;

b) X. Sun, S. R. Dawson, T. E. Parmentier, G. Malta, T. E. Davies, Q. He, L. Lu, D. J. Morgan, N. Carthey, P. Johnston, S. A. Kondrat, S. J. Freakley, C. J. Kiely, G. J. Hutchings, *Nat. Chem.* **2020**, *12*, 560; c) Z. Chen, Y. Chen, S. Chao, X. Dong, W. Chen, J. Luo, C. Liu, D. Wang, C. Chen, W. Li, J. Li, Y. Li, *ACS Catal.* **2020**, *10*, 1865.

[5] P. Johnston, N. Carthey, G. J. Hutchings, *J. Am. Chem. Soc.* **2015**, *137*, 14548.

[6] L. Ye, X. Duan, S. Wu, T. S. Wu, Y. Zhao, A. W. Robertson, H. L. Chou, J. Zheng, T. Ayvali, S. Day, C. Tang, Y. L. Soo, Y. Yuan, S. C. E. Tsang, *Nat. Commun.* **2019**, *10*, 914.

[7] M. Zhu, Q. Wang, K. Chen, Y. Wang, C. Huang, H. Dai, F. Yu, L. Kang, B. Dai, *ACS Catal.* **2015**, *5*, 5306.

[8] M. Conte, A. Carley, G. Attard, A. Herzing, C. Kiely, G. Hutchings, *J. Catal.* **2008**, *257*, 190.

[9] S. K. Kaiser, R. Lin, F. Krumeich, O. V. Safonova, J. Pérez-Ramírez, *Angew. Chem., Int. Ed.* **2019**, *58*, 12297.

[10] S. K. Kaiser, E. Fako, G. Manzocchi, F. Krumeich, R. Hauert, A. H. Clark, O. V. Safonova, N. López, J. Pérez-Ramírez, *Nat. Catal.* **2020**, *3*, 376.

[11] L. Zhang, R. T. Si, H. S. Liu, N. Chen, Q. Wang, K. Adair, Z. Q. Wang, J. T. Chen, Z. X. Song, J. J. Li, M. N. Banis, R. Y. Li, T. K. Sham, M. Gu, L. M. Liu, G. A. Botton, X. L. Sun, *Nat. Commun.* **2019**, *10*, 4936.

[12] B. B. Sarma, J. Kim, J. Amsler, G. Agostini, C. Weidenthaler, N. Pfander, R. Arenal, P. Concepcion, P. Plessow, F. Studt, G. Prieto, *Angew. Chem., Int. Ed.* **2020**, *59*, 5806.

[13] S. Feng, X. Song, Z. Ren, Y. Ding, *Ind. Eng. Chem. Res.* **2019**, *58*, 4755.

[14] M. J. Richardson, J. H. Johnston, T. Borrmann, *Eur. J. Inorg.Chem.* **2006**, *2006*, 2618.

[15] E. Vorobyeva, E. Fako, Z. Chen, S. M. Collins, D. Johnstone, P. A. Midgley, R. Hauert, O. V. Safonova, G. Vile, N. López, S. Mitchell, J. Pérez-Ramírez, *Angew. Chem., Int. Ed.* **2019**, *58*, 8724.

[16] a) R. F. Egerton, M. Watanabe, *Ultramicroscopy* **2018**, *193*, 111; b) K. Suenaga, M. Tence, C. Mory, C. Colliex, H. Kato, T. Okazaki, H. Shinohara, K. Hirahara, S. Bandow, S. Iijima, *Science* **2000**, *290*, 2280.